Cell PRESS
Developmental Cell
Article

Latrophilin Signaling Links Anterior-Posterior Tissue Polarity and Oriented Cell Divisions in the *C. elegans* Embryo

Tobias Langenhan,[1,5] Simone Prömel,[1] Lamia Mestek,[1] Behrooz Esmaeili,[1,6] Helen Waller-Evans,[1] Christian Hennig,[2] Yuji Kohara,[3] Leon Avery,[4] Ioannis Vakonakis,[1,7] Ralf Schnabel,[2] and Andreas P. Russ[1,*]
[1]Department of Biochemistry, University of Oxford, Oxford OX1 3QU, UK
[2]Institut für Genetik, TU Braunschweig, 38106 Braunschweig, Germany
[3]Genome Biology Laboratory, National Institute of Genetics, Mishima 411-8560, Japan
[4]Department of Molecular Biology, University of Texas Southwestern Medical Center, Dallas, TX 75390-9148, USA
[5]Present address: Institute of Physiology, University of Würzburg, 97070 Würzburg, Germany
[6]Present address: School of Graduate Entry Medicine and Health, University of Nottingham, Royal Derby Hospital, Derby DE22 3DT, UK
[7]Present address: Paul Scherrer Institut, 5232 Villigen PSI, Switzerland
*Correspondence: andreas.russ@bioch.ox.ac.uk
DOI 10.1016/j.devcel.2009.08.008

SUMMARY

Understanding the mechanisms that coordinate the orientation of cell division planes during embryogenesis and morphogenesis is a fundamental problem in developmental biology. Here we show that the orphan receptor *lat-1*, a homolog of vertebrate latrophilins, plays an essential role in the establishment of tissue polarity in the *C. elegans* embryo. We provide evidence that *lat-1* is required for the alignment of cell division planes to the anterior-posterior axis and acts in parallel to known polarity and morphogenesis signals. *lat-1* is a member of the Adhesion-GPCR protein family and is structurally related to *flamingo/CELSR*, an essential component of the planar cell polarity pathway. We dissect the molecular requirements of *lat-1* signaling and implicate *lat-1* in an anterior-posterior tissue polarity pathway in the pre-morphogenesis stage of *C. elegans* development.

INTRODUCTION

While substantial progress has been made to identify the molecular mechanisms establishing cell polarity (reviewed in Gönczy, 2008; Siller and Doe, 2009), it is less well understood how polarity is propagated in tissues and coordinated with morphogenetic movements (reviewed by Zallen, 2007). The invariant embryonic cell lineage of the nematode *C. elegans* is defined by a sequence of precisely controlled asymmetric cell divisions and intercellular induction events that coordinate cell fates and cell division planes in an anterior-posterior (a-p) orientation (Kaletta et al., 1997; Lin et al., 1998; Priess, 2005; Schnabel, 1997; Sulston et al., 1983). The *wnt*/β-catenin asymmetry pathway has been shown to be essential for cell fate decisions (reviewed by Mizumoto and Sawa, 2007), while a noncanonical *wnt/frizzled* (*wnt/fz*) pathway is required for the orientation of mitotic spindles (reviewed by Walston and Hardin, 2006). The mechanisms controlling cell polarity in the first, second, and third rounds of embryonic cell divisions are understood in considerable detail (Gönczy and Rose, 2005; Walston and Hardin, 2006). A posterior polarizing center is located in the descendants of the founder blastomere P_1 (Hutter and Schnabel, 1995b) and can orient the division planes of immediately adjacent cells (Goldstein, 1995). The polarization of EMS by P_2 at the four-cell stage is thought to require an instructive *wnt/fz* signal and a permissive activity of *src-1/mes-1* (Bei et al., 2002; Goldstein et al., 2006; Rocheleau et al., 1997; Schlesinger et al., 1999; Thorpe et al., 1997; Walston et al., 2004). However, it is not well understood how the polarizing information is propagated and coordinated as the complexity of the embryo increases rapidly from the fourth to the tenth division cycle. A *wnt*-dependent relay mechanism has been proposed (Bischoff and Schnabel, 2006), but it is not clear how this mechanism relates to existing models for planar cell polarity (PCP) or a-p tissue polarity signaling (Park and Priess, 2003; Park et al., 2004).

An interesting family of candidate molecules for the control of cell-cell interactions are the Adhesion-GPCRs, a receptor class combining extracellular domain features of adhesion molecules with transmembrane regions characteristic for G-protein-coupled receptors. Vertebrate genomes encode 30 or more Adhesion-GPCRs with at least 8 different extracellular domain architectures (Nordström et al., 2008), making it the second largest group of seven-pass transmembrane (7TM) receptors. Adhesion-GPCRs are implicated in immune functions (Veninga et al., 2008) and in rare inherited developmental disorders (e.g., Piao et al., 2004), but their physiological functions remain very poorly understood.

The currently best known Adhesion-GPCRs are the cadherin-like *flamingo/starry night* (FMI) and its vertebrate homologs (CELSR), which have essential and conserved functions in the PCP pathway and in neuronal development (Chae et al., 1999; Curtin et al., 2003; Hadjantonakis et al., 1998; Lawrence et al., 2007; Shima et al., 2004; Strutt, 2008; Tissir et al., 2005; Usui et al., 1999). Comparative genomics of the highly divergent Adhesion-GPCR family shows that next to FMI only the domain architecture of latrophilins is strictly conserved across phyla

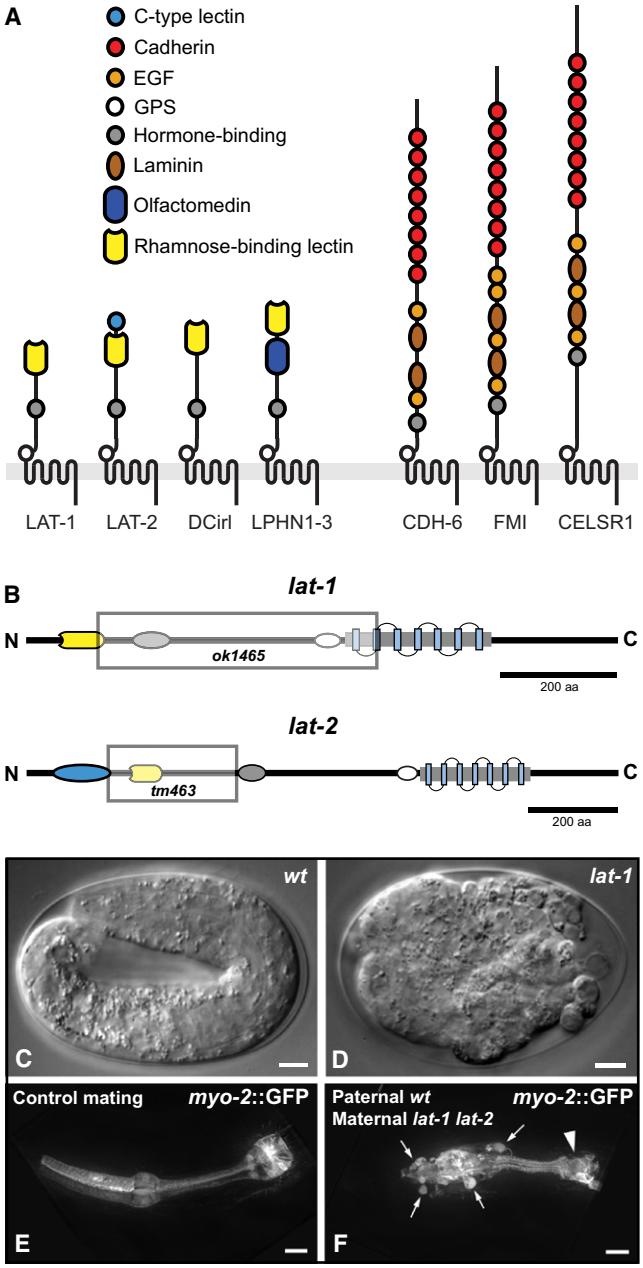

Figure 1. Evolutionary Conservation and Mutant Phenotype of *lat-1*

(A) Domain architectures of LPHN and FMI proteins. *C. elegans*: LAT-1, LAT-2, CDH-6; *Drosophila*: DCirl, FMI; *Homo sapiens*: LPHN1-3, CELSR1-3.

(B) Mutant alleles used in this study. Shaded boxes represent the genomic deletions in *lat-1(ok1465)* and *lat-2(tm463)*.

(C–F) Embryonic defects of latrophilin single mutants. (C) Elongated WT larva at pretzel stage. (D) A *lat-1(ok1465)* mutant lacking maternal and zygotic gene product. (E and F) Maternal effect of *lat-1(ok1465)*. (C) Control larva heterozygous for *myo-2p::gfp* transgene. (D) Heterozygous offspring of homozygous *lat-1* hermaphrodite. Ectopic pharyngeal cells (arrows) are labeled by paternally derived *myo-2p::gfp* and do not integrate into the pharynx; arrowhead: terminal bulb. Scale bars in (C) and (D) = 5 μm, in (E) and (F) = 10 μm.

(Nordström et al., 2008). The lectin-like latrophilins (LPHN; synonyms CL/CIRL/Lph) were originally described as cellular receptors for latrotoxin, the main neurotoxin of the black widow spider *Latrodectus mactans* (Krasnoperov et al., 1997), and implicated as modulators of neurotransmitter release (Südhof, 2001; Willson et al., 2004). However, their physiological functions are not understood. Here we demonstrate that LPHN signaling is required for the coordination of a-p tissue polarity and the alignment of cell division planes in the early *C. elegans* embryo.

RESULTS

Maternal and Zygotic *lat-1* Expression Is Required for *C. elegans* Development

The *C. elegans* genome contains two LPHN genes, *lat-1* and *lat-2* (Mee et al., 2004; Willson et al., 2004), and a single FMI homolog, *cdh-6* (Hutter et al., 2000). Similarly, FMI and LPHN (dCIRL) are the only conserved Adhesion-GPCR architectures in *Drosophila* (Figure 1A). Other *C. elegans* or *Drosophila* genes predicted to encode GPCR proteolytic site (GPS) and seven-pass transmembrane (7TM) domains are highly divergent, with little sequence homology to vertebrate Adhesion-GPCRs (Nordström et al., 2008).

In the mutant allele *lat-1(ok1465)* most of the protein coding region is deleted (Figure 1B). Heterozygous hermaphrodites have no obvious phenotype and produce broods of normal size. They segregate homozygous *lat-1(ok1465)* larvae at the expected Mendelian ratio, 99% of which arrest at the L1 stage (Guest et al., 2007). The mutant larvae are not paralyzed and embryonic lethality is not observed (Table 1).

A small fraction (~1%) of *lat-1(ok1465)* larvae escape the L1 arrest, and slow-growing homozygous populations can be maintained (see Figure S1 available online) (Guest et al., 2007). Offspring of homozygous hermaphrodites display embryonic lethality and variable morphogenetic defects in L1 larvae and adult stages, new phenotypes that are not observed in homozygous offspring of heterozygous hermaphrodites (Figures 1C and 1D; Table 1). Mating of homozygous *lat-1(ok1465)* hermaphrodites with heterozygous *lat-1(ok1465)*/+ males reveals maternal-effect lethality in heterozygous *lat-1(ok1465)*/+ offspring (Figures 1E and 1F; Table 1), indicating that maternal *lat-1* is required for embryonic development.

lat-1(ok1465) Is a Null or Strong Loss-of-Function Allele

We tested whether *lat-1(ok1465)* is a null allele or a hypomorphic mutation, and if *lat-1* and the paralog *lat-2* have overlapping functions. Our results indicate that *lat-1(ok1465)* is a strong loss-of-function or null allele: (1) the coding regions for all protein domains are deleted or truncated, so that a hypothetical mutant protein would only consist of an incomplete GPCR-like domain with six transmembrane helices (Figure 1B); (2) we were not able to detect residual protein or transcript; (3) the phenotype of *lat-1(ok1465)* in *trans* to a chromosomal deficiency is indistinguishable from homozygous *lat-1(ok1465)*; and (4) RNA-mediated interference (RNAi) of *lat-1* does not enhance the *lat-1(ok1465)* phenotype (data not shown).

Strains homozygous for *lat-2(tm463)* have no obvious phenotype (Figure S1) (Guest et al., 2007; Willson et al., 2004). In *lat-2(tm463)* the extracellular domain is partially deleted (Figure 1B), and we could not detect residual transcript, suggesting that *lat-2(tm463)* is a loss-of-function allele. The double-mutant strain *lat-1(ok1465) lat-2(tm463)* shows enhanced penetrance

Table 1. Frequency of Embryonic and Larval Arrest Phenotypes Depending on Maternal and Zygotic Genotype for *lat-1* and *lat-2*

Strain/Mating	Maternal Genotype	Zygotic Genotype	Embryonic Arrest [%]	L1 Arrest [%]	N (Sets)
N2	+/+	+/+	0.6 ± 0.4	0.6 ± 0.6	1513 (5)
lat-1(ok1465)	−/−	−/−	16.8 ± 2.5	55.5 ± 2.4	1789 (8)
lat-2(tm463)	−/−	−/−	0.5 ± 0.5	3.6 ± 3.6	395 (3)
lat-1(ok1465) lat-2(tm463)	−/−	−/−	24.2 ± 3.3	73.4 ± 3.4	1026 (4)
lat-1(ok1465)/mIn1[mIs14 dpy-10(e128)]	+/−	mendelian +/+, +/−, −/−	1.0 ± 0.2	26.3 ± 0.8	1004 (6)
lat-1(ok1465) mated to WT males	−/−	+/−	5.6 ± 0.6	1.5 ± 0.8	1058 (3)
lat-1(ok1465) lat-2(tm463) mated to *mIn1* males	−/−	++/−−	11.9 ± 0.9	4.5 ± 0.9	1096 (3)
mom-2(t2180ts) (25°C)	−/−	−/−	99.7 ± 0.1	0.3 ± 0.1	2078[a] (3)
mom-2(t2180ts) (15°C)	−/−	−/−	4.6 ± 0.6	1.7 ± 0.5	2028[a] (3)
lat-1(ok1465); mom-2(t2180ts) (15°C)	−/−;−/−	−/−;−/−	>95.0	<5.0	1209[a] (2)
lat-1(ok1465) lat-2(tm463); mom-2(t2180ts) (15°C)	−/−;−/−	−/−;−/−	>98.0	<2.0	872[a] (2)

Line 5 shows the numbers for the offspring of heterozygous hermaphrodites carrying a balancer chromosome with an expected Mendelian frequency of 25% for homozygous mutants. Preselection of homozygous larvae by lack of balancer chromosome leads to indistinguishable results. Experimental spread is indicated as SEM.

[a] *mom-2(t2180ts)* numbers obtained from pooled progeny of three mothers per plate.

of the late embryonic and larval defects seen in *lat-1(ok1465)*, but no qualitative change to the early embryonic phenotype (Table 1; Figure S1). These results indicate that there is partial overlap between *lat-1* and *lat-2* function, but that only *lat-1* is required for normal development. We subsequently refer to the alleles just as *lat-1* and *lat-2*.

lat-1 Is Expressed during Oogenesis, Embryogenesis, and Organogenesis

Consistent with the maternal effect, *lat-1* mRNA is detected in the gonad during oogenesis and in the blastomeres of the early embryo (Figures 2A and 2B). The expression of *lat-1* reporter constructs starts with the onset of zygotic transcription and is initially stronger in the AB lineage than in P_1-derived blastomeres (Figure 2C). Before the onset of overt morphogenesis, *lat-1* is widely expressed in epidermal and pharyngeal precursors and shows a reproducible left-right asymmetry in the epidermal primordium, which results in a striped pattern during dorsal intercalation (Figures 2E, 2G, and 2H). In larval and adult stages, *lat-1* is expressed in the pharynx, the nervous system, the gonad, and the vulva (data not shown). The expression of *lat-2* largely overlaps with *lat-1* in the pharyngeal primordium (Figure 2F) and remains confined to the pharynx and the excretory cell in later stages.

The expression of wild-type LAT-1 protein or a LAT-1::GFP fusion protein under the control of *lat-1* regulatory regions efficiently rescues the mutant phenotype (Figure 2D; Figures S1 and S2). Immunohistochemical detection with antibodies raised against the LAT-1 N-terminal RBL domain confirms the localization of the protein to the cell membrane (Figure 2H). The endogenous expression level of LAT-1 in embryos is very low, and the protein can only be detected in strains expressing a rescuing transgenic array.

Zygotic expression of *lat-1* in the pharynx primordium provides only partial rescue (Figure S1), and expression under an epidermis-specific promoter results in increased embryonic lethality. Conditional expression of LAT-1 under a heat-shock promoter disrupts the morphogenesis of wild-type embryos (data not shown), confirming that LAT-1 protein levels are under tight spatial and temporal control.

The defining feature of latrophilin-like receptors is the highly conserved RBL (*r*hamnose-*b*inding *l*ectin) domain (Vakonakis et al., 2008). The rescuing activity of *lat-1* transgenes is absolutely dependent on the presence of the RBL domain, although we could not detect any carbohydrate-binding activity (Figure S1 and S2). Constructs expressing membrane-tethered RBL domains or secreted N-terminal fragments of *lat-1* were also inactive (Figure S2).

Maternal *lat-1* Is Required for the Correct Localization of the ABala Blastomere

To understand the function of *lat-1* in early development, we observed blastomere divisions by 4D microscopy (Schnabel et al., 1997) and traced the embryonic cell lineages in *lat-1* and *lat-1 lat-2* mutants. Cell fates and the orientation of division planes in the AB and P_1 lineage were normal up to the eight-cell/AB^4 stage (Figure 3; Figures S3–S5). However, in the fourth round of cell divisions, we detected a specific change to the cleavage plane of the ABal blastomere that consistently alters the position of ABala.

In wild-type embryos, ABal divides in an a-p direction (Figures 3A, 3C, and 3E). Due to the space constraints within the eggshell, the division plane is tilted relative to the theoretical a-p axis (Bischoff and Schnabel, 2006), but daughter cells are placed in a stereotypical a-p pattern. Only the posterior daughter ABalp remains in contact with the MS blastomere, while the anterior daughter ABala moves to the most anterior position in the embryo. An inductive interaction between ABalp and MS based on *glp-1*/Notch signaling triggers the ABalp lineage to adopt pharyngeal cell fates (Hutter and Schnabel, 1994; Mango et al., 1994; Priess et al., 1987). In contrast, ABala does not contact MS, and the ABala lineage retains neuronal fate (Figures 3A and 3C).

In embryos lacking maternal *lat-1* gene product, the orientation of the ABal division plane is perpendicular to the a-p axis.

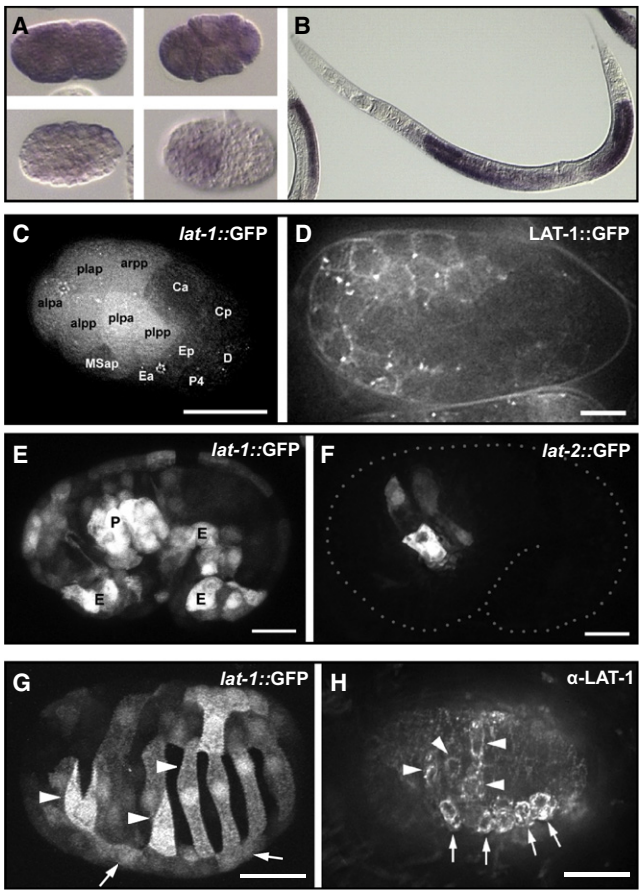

Figure 2. Expression Pattern of *lat-1* and *lat-2*

(A) *lat-1* mRNA in early blastomeres and (B) the gonad detected by in situ hybridization. (C and D) Zygotic expression of *lat-1* in early embryonic development.

(C) Expression of a *lat-1p::gfp* reporter gene at 26-cell stage. AB descendants are labeled "alaa" for ABalaa, etc.

(D) Membrane localization of a rescuing in-frame LAT-1::GFP fusion protein, 200-cell stage.

(E and F) Expression of *lat-1* and *lat-2* overlaps in the pharynx primordium. (E) *lat-1p::gfp* expression with strong signal in the pharyngeal primordium ("P") and ventral epidermal precursors ("E"). (F) *lat-2p::gfp* expression at the same stage is confined to the pharynx primordium.

(G and H) Asymmetric expression of *lat-1* in epidermal precursors during dorsal intercalation visualized with a *lat-1p::gfp* transgene (G) or by detection with an α-LAT-1 antibody. Arrows indicate position left seam cells, and arrowheads mark LAT-1-positive intercalating left dorsal epidermal cells. Scale bars in (C), (G), and (H) = 10 μm, in (D), (E), and (F) = 5 μm.

Both ABalp and ABala retain equal contact to MS after the division, and ABala is not displaced toward the anterior (Figures 3B, 3D, and 3F). This phenotype is highly penetrant and dependent on the absence of maternal *lat-1* gene product (Table 2). It is clearly distinct from the effect of mutations disrupting *wnt* signaling, which change the division plane of ABar so that ABarp instead of ABara contacts MS, but do not result in contact of ABala with MS (Figures S3A and S3B) (Rocheleau et al., 1997; Schlesinger et al., 1999; Thorpe et al., 1997; Walston et al., 2004). In *lat-1* mutants, the division plane of ABar is oriented toward C and similar to the wild-type orientation (Figures S3C and S3D), although minor effects might be obscured by the changes in the ABal division plane.

lat-1 Is Required for the Alignment of ABal and MS Spindles

We used GFP::β-tubulin fusion proteins to visualize spindle alignment during blastomere divisions in real time (Strome et al., 2001). In the absence of maternal and zygotic *lat-1*, the asymmetry of the P_0 division and the spindle orientations of the AB, P_1, P_2, EMS, ABa/p, E, and C blastomeres are unaffected (Figure 3; Figures S4 and S5). Changes are first observed in the late eight-cell/AB^4 stage during the alignment of ABal and MS spindles.

In both wild-type and *lat-1* embryos, the AB^4 centromeres duplicate 2–4 min before MS and E centromeres. In controls, the posterior spindle pole of ABal and the anterior spindle pole of MS come into close apposition (average distance 8.7 μm, n = 12). In *lat-1* embryos, ABal and MS spindle poles do not move into apposition (average distance 12.7 μm, n = 33), and the ABal spindle aligns perpendicular to the MS spindle (Figures 3E and 3F).

The timing of MS spindle alignment is disrupted in 60% of *lat-1* mutants (Figure 3; Table 2), and in rare cases MS divides in a left-right (l-r) instead of a-p orientation (1/30, Figure S5). In controls, the a-p alignment of E, MS, and ABal is tightly coordinated and occurs synchronously, while in *lat-1* mutants the MS spindle "wobbles" and a-p alignment is delayed until the division of ABal is completed (Figures 3F and 3H; Table 2). The a-p alignment of E and C blastomeres is unaffected, indicating that *lat-1* is specifically required for the alignment of ABal and MS spindles.

Like the division plane defects of ABal and ABar, the delayed orientation of the MS spindle in *lat-1* is a phenotype similar, but not identical, to the effect of mutations disrupting the *wnt* pathway. There, the alignment of the EMS spindle is delayed, but EMS eventually divides in the a-p orientation (Bei et al., 2002; Schlesinger et al., 1999; Walston et al., 2004). If *lat-1* was carrying a second instructive a-p signal, the combined disruption of *wnt/fz* and *lat-1* function might abolish alignment of blastomeres to the a-p axis and result in random division plane orientations (Gotta and Ahringer, 2001). To test this model, we constructed double mutants lacking maternal and zygotic gene products for *lat-1* and the *wnt* homolog *mom-2(or42)* or the *frizzled* homolog *mom-5(zu193)*, respectively. We found that the frequency of tilted MS divisions was increased (tilted MS division percentage [n]: *mom-2*, 62% [13]; *lat-1;mom-2*, 93% [15]; *mom-5*, 17% [12]; *lat-1/mom-5*, 60% [5]), but that a-p polarity of EMS and E divisions was retained (data not shown). We did not observe left-right divisions of EMS in *lat-1/mom* mutants, as they have been described to occur with high penetrance in *mom/src* double mutants (Bei et al., 2002).

The effects of *lat-1* on ABal and *mom-2/mom-5* on ABar division plane orientation were additive in double mutants, and randomization of AB division planes was not observed. These results suggest that *lat-1* is acting in parallel to *mom-2/mom-5* signaling. They are also consistent with our findings in single mutants, which indicate that *lat-1* is not required for $P_2 \rightarrow$EMS or C→ABar signaling (Walston et al., 2004).

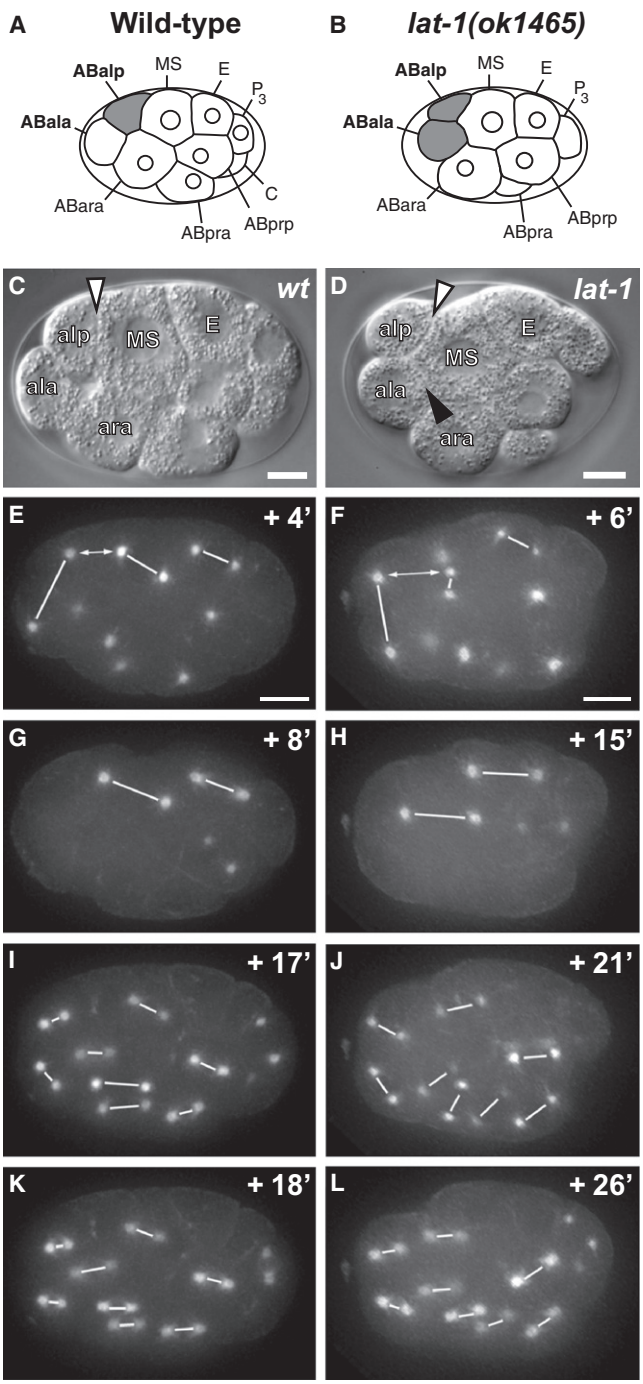

Figure 3. Division Plane Defects of *lat-1* Mutants

Left column, WT embryo; right column, *lat-1* embryo. (C and D) DIC microscopy; (E–L) spindle orientation visualized by GFP::β-tubulin. Centromere pairs are linked with white lines. Time points are shown in minutes relative to AB^4 stage (Figures S3C and S3D). (A–D) Relative positions of ABala, ABalp, and MS in WT (A and C) and *lat-1* (B and D) embryos. Note that in *lat-1* ABala forms an extensive membrane interface with MS (black arrowhead in [D]). (E) a-p alignment of ABal and MS spindles in WT embryo. (F) In *lat-1* embryo a-p spindle alignment fails in ABal and is delayed in MS. a-p alignment of E precedes MS. The distance between the posterior ABal centromere and anterior MS centromere is marked by double arrows. (G and H) Delayed a-p alignment of MS spindle in mutant (H) compared to WT (G). (I–L) Rapid a-p alignment of AB^8 spindles in WT embryos (I and K). Delayed alignment in *lat-1* embryos (J and L) and perpendicular division planes of sister cells. In all embryos anterior is to the left, posterior is to the right, and ventral (MS) is up. Scale bars = 5 μm.

lat-1 Acts after the 12-Cell Stage to Provide Robust a-p Orientation

Zygotic *lat-1* activity is also required for spindle alignment after the fourth round of cell divisions. In the fifth round of cell divisions, spindle alignment is rapid and robust in wild-type embryos, and ABala and ABalp daughters arrange in a parallel a-p orientation. In 50% of *lat-1* specimens, ABala/p show delayed alignment or perpendicular division (Figures 3J and 3L; Figure S4D; Table 2). The quantitative evaluation of cell divisions by 4D recording (Bischoff and Schnabel, 2006; Schnabel et al., 1997) confirms the persistence of this phenotype up to the eighth round of divisions. The majority of cells in *lat-1* embryos divide in a-p orientation, but an apparently stochastic failure of a-p division plane orientation is observed (Figure S6).

The fact that in *lat-1* mutants a-p alignment is delayed, but not abolished, indicates that another pathway carries a-p information. A good candidate is *mom-2*/wnt, which has been suggested to provide a-p information by means of a cellular relay mechanism (Bischoff and Schnabel, 2006). To test if the late a-p alignment of ABaxx cells is dependent on *mom-2* signaling, we generated double mutant lines for *lat-1* and the temperature-sensitive *wnt* allele *mom-2(t2180ts)* (Bischoff and Schnabel, 2006). *mom-2(t2180ts)* single homozygotes display only mild lethality at the permissive temperature, indicating that the allele retains significant activity (Table 1). However, we were not able to perform the intended temperature shift experiment, as *lat-1; mom-2(t2180ts)* double mutants show nearly complete embryonic lethality at the permissive temperature and can hardly be propagated (Table 1). The strong overadditive effect of a weak hypomorphic *mom-2* allele with *lat-1* is consistent with activity in parallel pathways or with a role for *lat-1* in the efficient propagation of the *mom-2* signal.

An important feature of *lat-1* mutants is a variable defect in epidermal morphogenesis. We could visualize the abnormal placement of epidermal seam cells (Figures 4A and 4B) and were able to detect errors in division-plane alignment in the ABarpp sublineage by 4D microscopy (Figures 4C and 4D). These defects preceded the migration of seam cell precursors to their lateral positions, suggesting a direct link between the molecular and cellular function of *lat-1* in division plane alignment and the phenotypic outcome on the level of tissue morphogenesis.

Indirect Transformation of Cell Fates in *lat-1* Mutants

In the *C. elegans* embryo, the determination of cell fate by asymmetric cell divisions and the control of a-p orientation are regulated by different branches of the *wnt* pathway (Mizumoto and Sawa, 2007). This raises the question of whether *lat-1* signaling has direct effects on cell fate. In addition, the ectopic contact of ABala and MS in *lat-1* mutants predicts that a *glp-1*/Notch induction of ABala might lead to indirect, secondary effects on cell fate in the ABala lineage (Priess, 2005). We investigated

Table 2. Summary of AB and MS Spindle Alignment Defects in Latrophilin Mutants

Strain (Incubation Temperature)	Maternal Genotype	Zygotic Genotype	ABal Spindle Defect [% (n/Total)]	MS Orientation Delay [% (n/Total)]	ABalxx Delay [% (n/Total)]	ABalxx Defect [% (n/Total)]
N2 (25°C)	+/+	+/+	0 (0/6)	0 (0/6)	0 (0/6)	N.A.
N2 (20°C)	+/+	+/+	0 (0/12)	0 (0/12)	0 (0/12)	N.A.
lat-1(ok1465)/mIn1 [mIs14 dpy-10(e128)] (25°C)	+/−	+/+, +/−	0 (0/10)	N.D.	N.D.	N.D.
lat-1(ok1465)/mIn1 [mIs14 dpy-10(e128)] (25°C)	+/−	−/−	0 (0/5)	N.D.	N.D.	N.D.
lat-1(ok1465); Ex[lat-1(+)] (25°C)	−/−; *Ex[lat-1(+)]*	−/−; *Ex[lat-1(+)]*	75 (3/4)[a]	N.D.	N.D.	N.D.
lat-1(ok1465) (25°C)	−/−	−/−	100 (17/17)	N.D.	N.D.	N.D.
lat-1(ok1465) lat-2(tm463) (25°C)	−/−	−/−	100 (14/14)	N.D.	N.D.	N.D.
lat-1(ok1465) mated to WT male (25°C)	−/−	+/−	100 (4/4)	N.D.	N.D.	N.D.
lat-1(ok1465) (20°C)	−/−	−/−	75 (42/56)	59 (10/17)	47 (7/15)	33 (5/15)
lat-1(ok1465) lat-2(tm463) (20°C)	−/−	−/−	67 (10/15)	60 (9/15)	53 (8/15)	27 (4/15)

N.D., not determined; N.A., not applicable.
[a] 2/4 animals hatched. This number is an underestimate of the ABal spindle defect rescuing capacity of *Ex[lat-1(+)]* due to array loss and low transgene expression in the maternal germline.

cell fate by analysis of cell lineage and the expression of differentiation markers.

We did not observe E↔MS cell fate transformations or atypical cell death events in the MS lineage as described for the *wnt*/β-catenin asymmetry pathway (Rocheleau et al., 1997; Thorpe et al., 1997). The majority of *lat-1* embryos express the marker *lag-2p::gfp* in a wild-type pattern in ABala daughters (93% [n = 71], control 100% [n = 87]), indicating that the ABala lineage fate is retained in spite of the change in division plane and close contact to an inducing signal from MS (Figures 5A and 5B). We were unable to find unambiguous evidence to indicate that the observed errors in a-p division plane alignment are linked to random a↔p cell fate transformations (Figure S7) (Huang et al., 2007; Kaletta et al., 1997).

In contrast, we could readily detect the secondary effects of altered cell contacts on Delta/Notch induction events. At low-frequency, we detect the displacement (3%) or absence (4%) of ABala-derived *lag-2p::gfp* expressing cells, the expected result of "illegitimate" induction of ABala by MS (Figure 5C). The ABala-derived *lag-2* signaling center is in turn required for the induction of epidermal fate in the ABplaaa lineage. Its absence leads to the characteristic "twisted head" phenotype (Lambie and Kimble, 1991), which can be observed in *lat-1* at the expected frequency (data not shown).

We could detect the absence of programmed cell death events in the ABala and ABalp lineage in five out of six mutant embryos analyzed (Figure S7). Immunohistochemical staining of differentiated pharyngeal muscle cells with the monoclonal antibody 3NB12 shows a wide variation in the number of marker-positive cells (Figures 5D–5F), a finding consistent with "mosaic" changes of distal lineage branches (Hutter and Schnabel, 1995a; Rocheleau et al., 1997; Thorpe et al., 1997) rather than full transformation of ABala to another ABaxx lineage fate. Our results strongly suggest that, in spite of the reorientation of the division plane, the ABal division in *lat-1* embryos is still asymmetric (Figure S7) (Gomes et al., 2001) and that *lat-1* signaling is not directly coupled to cell fate asymmetry in a-p divisions.

DISCUSSION

lat-1 Is Required for Cell Division Plane Orientation in the *C. elegans* Embryo

This study provides evidence that the orphan receptor *lat-1* plays an essential role in the alignment of cell division planes during the early embryonic development of *C. elegans*. We show that both maternal and zygotic expression of *lat-1* are essential for normal development, and identify changes of division plane orientation as a fully penetrant cellular phenotype in *lat-1* mutants. The altered cell positions and the resulting secondary effects on inductive cell-cell interactions, e.g., via "illegitimate" *glp-1*/Notch signaling, contribute to the variable morphogenetic abnormalities of *lat-1* mutants.

The investigation of mitotic spindle orientation in the *C. elegans* embryo has identified the roles of PAR proteins and heterotrimeric G proteins in establishing zygotic polarity (Gönczy and Rose, 2005), and of the *wnt/fz* and *src-1/mes-1* pathways in P_2/EMS signaling at the four-cell stage (Walston and Hardin, 2006). However, it is still poorly understood how spindle orientation and cell fate asymmetry are coordinated from the eight-cell stage onward. Clear equivalents of PCP or a-p tissue polarity pathways have not yet been defined in *C. elegans* embryogenesis (Park et al., 2004; Walston et al., 2004). Our results suggest that *lat-1* acts in an a-p tissue polarity pathway in the *C. elegans* embryo.

Evidence for a *lat-1*-Dependent a-p Tissue Polarity Pathway in *C. elegans*

We show that *lat-1* is essential to align the mitotic spindles and division planes of the E-MS-ABal cell group to a common a-p axis. In *lat-1* mutants, the alignment of the MS spindle is delayed in ~50% and fails in ~5% of the embryos we observed. The timing of spindle rotations suggests that successful alignment of E can "rescue" the alignment defect of MS, but not ABal, which has already undergone mitosis at this time. While lack of *lat-1* function has little or no effect on the division planes of blastomeres that are in direct contact with the primary or secondary

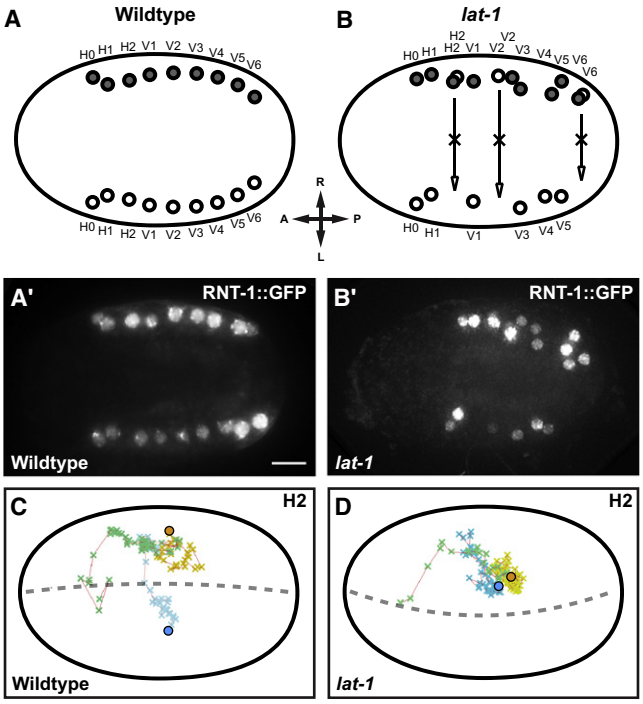

Figure 4. Seam Cell Positioning Defects in *lat-1* Mutants

(A and A′) The seam cell marker RNT-1::GFP labels two seam cell rows of ten cells each on either side of WT embryos.

(B and B′) RNT-1-positive cells persist on the right side in *lat-1* mutant.

(C and D) The migration path of H2 seam cells and their precursors was traced by 4D microscopy. Green, migration path of common ABarpp precursors. Movement of ABarpp descendants after left-right split of cell lineage: blue, left descendants (ABarppax); yellow, right descendants (ABarpppx); spheres, final destination of differentiated seam cells. (C) Contralateral migration of H2L/H2R in WT embryo. (D) In a *lat-1* embryo left-right migration is absent, and H2L and H2R stay together. Dorsal views, anterior to the left. Scale bar = 5 μm.

signaling cells $P_{2/3}$, E, and C, spindle alignment in ABal or ABarp descendants is frequently delayed or failing. Our results can be accommodated in a simple model in which *lat-1* is required to efficiently propagate spindle alignment cues from a posterior source to more anterior cells in the growing cellular array. In this model, ABal is a weak spot for at least two reasons. First, its orientation is completely dependent on MS (Park and Priess, 2003), a "tertiary" signaling cell that is not in direct contact to P_2 and shows delays and errors of a-p orientation in *lat-1* mutants. Second, ABal has fewer spatial constraints that could bias the orientation of its division plane than later ABa-derived blastomeres, which have more diverse cell contacts that could provide compensating signals.

lat-1 Interacts Genetically with the *wnt* Spindle Orientation Pathway

The analysis of *mom-1*(porcupine)/*mom-2* double mutants suggests parallel *wnt* signals as the source of polarizing information (Rocheleau et al., 1997; Thorpe et al., 1997). *lat-1* might be required to propagate one of the parallel and partially redundant *wnt* signals, or an unknown *wnt*-independent signal. Alternatively, *lat-1* function might be needed for the efficient propagation of all parallel polarizing signals, e.g., by affecting an essential polarization response. Both possibilities would be consistent with the strong synergistic interaction of *lat-1* with a hypomorphic allele of *mom-2*/wnt. Alternative models are more complex, e.g., a *lat-1*-dependent anterior-to-posterior alignment activity opposing the *mom-2/5*-dependent posterior-to-anterior signal (Green et al., 2008). The laser ablation of MS does not support this model, as the spindle orientation of ABal in MS-ablated embryos resembles the orientation in *lat-1* mutants (R.S., unpublished data).

Our analysis of differentiation markers and embryonic cell lineages shows that *lat-1* is not required for endoderm induction and does not appear to have a strong direct effect on cell fate in asymmetric cell divisions even if a-p spindle orientation is changed. This indicates that *lat-1* is not an essential component of the *wnt*/β-catenin asymmetry pathway. In the majority of *lat-1* mutants, the ABal division still generates asymmetric cell fates. The normal ABala cell fate is surprisingly robust against the altered cell position and the ectopic cell contact to MS.

The role of *lat-1* in the epidermal ABarpp lineage is difficult to address. We demonstrate that, in the absence of *lat-1*, ABarpp descendants are correctly specified as seam cells expressing the *rnt-1* reporter gene. However, they do not migrate to left and right lateral positions but remain clustered near their "place of birth." The simplest model is that the migration of seam cell precursors is disrupted by defects in division plane alignment, while cell fate determination is unaffected. Alternatively, an error in cell fate specification might change ABarppa (left) cell fates into ABarppp (right) cell fates. As ABarppa/p lineage fates and marker gene expression are symmetrical to the l-r axis, we are currently unable to distinguish between these possibilities.

Comparison with PCP and Morphogenesis Pathways

We tested whether two other Adhesion-GPCRs in the *C. elegans* genome, *lat-2* and *cdh-6/fmi-1* (Hutter et al., 2000), interact genetically with *lat-1*. The LPHN paralog *lat-2* is expressed in a much more restricted pattern than *lat-1* and enhances lethality of the *lat-1* mutant. Our data are consistent with partially overlapping zygotic function in certain tissues (e.g., the pharynx), but indicate that *lat-2* is not required during early development.

The *cdh-6/fmi-1* mutant allele *tm306* has no obvious phenotype and does not enhance the latrophilin phenotypes in the double or triple mutants *lat-1; fmi-1* or *lat-1 lat-2; fmi-1*. The genomic deletion in *tm306* is small and may not result in a strong loss of function. We have not been able to achieve strong phenotypes by RNAi inhibition of *cdh-6/fmi-1* (Park et al., 2004) or other Adhesion-GPCRs, and a more detailed investigation of the interaction of *lat-1* and *cdh-6/fmi-1* will require the isolation of more mutant alleles.

The expression level of LAT-1 protein in the early embryo is below the limit of detection by our immunohistochemical assay that can detect endogenous expression levels at larval stages. The maternally deposited *lat-1* RNA is evenly distributed in the early embryo, but we have not been able to detect the localization of maternally encoded or deposited protein from the zygote to the 12-cell stage. Our current information about protein localization in the embryo is therefore based on transgenic expression and might be influenced by moderate overexpression. We could not find evidence for asymmetric subcellular distribution of LAT-1, which is in contrast to the asymmetric localization of

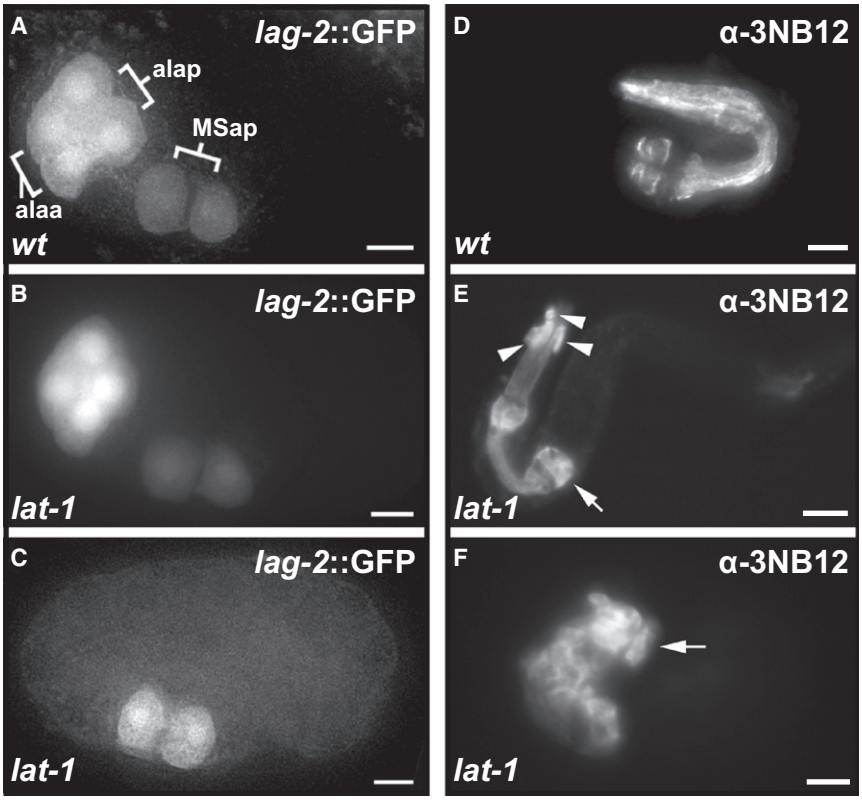

Figure 5. Cell Fate Transformations in Latrophilin Mutants

(A) MSap daughters and ABala granddaughters expressing *lag-2p::gfp* reporter gene in WT embryo.

(B) *lat-1* mutants typically express the *lag-2p::gfp* reporter gene in a WT configuration.

(C) In a minority of *lat-1* embryos, expression of *lag-2p::gfp* in the ABal lineage is absent or displaced. Lateral views, anterior to the left.

(D–F) α-3NB12 immunostaining of terminally differentiated pharyngeal muscle cells after pharynx elongation. Arrows indicate the terminal bulb. (D) WT larva, 21 3NB12$^+$ cells. (E) *lat-1* mutant larva with abnormal pharynx morphology and 25 3NB12$^+$ cells; the overall structure of the pharynx is preserved, but 3NB12$^+$ cells are displaced and extra cells are found in ectopic positions. (F) Mutant larva with a normal number of 21 3NB12$^+$ cells. The pharynx is disorganized and pharyngeal morphogenesis has failed. All scale bars = 5 μm.

PCP proteins in *Drosophila* (Strutt, 2008), but consistent with the observations in convergence and extension (C&E) and a-p tissue polarity models (Zallen, 2007). We consistently observe a left-right asymmetry of *lat-1* expression during epidermal morphogenesis, but have not detected defects in the handedness of *lat-1* mutant embryos.

The variable defects of morphogenesis in *lat-1* mutants might be entirely due to errors in division plane alignment. Alternatively, *lat-1* might have independent roles in the control of cell migration and morphogenesis. Morphogenetic defects are frequently described in mutants disrupting cell polarity, and a clean distinction from effects on morphogenesis might not be possible or meaningful. Genetic analysis indicates that latrophilin signaling acts in parallel to other signaling pathways controlling cell migration and morphogenesis, e.g., *vab-1*/ephR and *sax-3*/robo signaling (data not shown; unpublished data).

The Molecular Mechanism of Latrophilin Signaling

Adhesion-GPCRs are heterodimers composed of an extracellular "adhesion" subunit and a GPCR-like domain with seven transmembrane helices. The heterodimers are derived from monomeric precursor proteins by cleavage at the GPS domain (Krasnoperov et al., 1997; Lin et al., 2004), which is a defining feature of this receptor class. We find that the lectin-like RBL domain found in all LPHNs (Vakonakis et al., 2008) is absolutely required for the function of *lat-1*. In contrast to results recently described for FMI (Steinel and Whitington, 2009), constructs lacking the RBL domain but retaining the hormone-binding (HRM), GPS, and 7TM domains do not show partial activity. This is consistent with an essential role of the RBL domain in ligand binding and implies that the 7TM domain transduces an "outside-in" signal that is dependent on an extracellular interaction. Our biochemical data argue strongly against a carbohydrate ligand for the lectin-like RBL domain.

We were not able to complement the *lat-1* mutant phenotype with constructs expressing an N-terminal fragment containing only the RBL and stalk regions tethered to the cell surface with a single transmembrane helix instead of the GPS-7TM regions. This contrasts with recent reports that adhesive and signaling properties of FMI can be separated in zebrafish gastrulation (Carreira-Barbosa et al., 2009). We further tested for possible non-cell-autonomous functions by expressing the N-terminal fragment that might be released from the cell surface by cleavage at the GPS site, but were also unable to detect rescuing activity. These results suggest that *lat-1* acts cell-autonomously by detecting the interaction of the extracellular RBL domain with adjacent cells, extracellular matrix, or unknown ligands.

Outlook

Unexpectedly, this study reveals that the putative neurotoxin receptor *lat-1* defines a mechanism required for the alignment of cell division planes in *C. elegans* embryogenesis. Similar to studies showing the role of FMI in PCP (Lawrence et al., 2007; Zallen, 2007), our results implicate a second evolutionarily conserved subfamily of Adhesion-GPCRs in the control of tissue polarity and morphogenesis and suggest that the expansion of Adhesion-GPCRs in vertebrates might contribute to the larger variety of organ and tissue architectures (Curtin et al., 2003; Davies et al., 2004; Piao et al., 2004; Tissir et al., 2005). Further studies will be required to define the up- and downstream components of Adhesion-GPCR signaling.

EXPERIMENTAL PROCEDURES

C. elegans Strains

C. elegans strains were cultured and manipulated according to standard protocols (Brenner, 1974). Wild-type worms were *C. elegans* variety Bristol,

N2. *lat-1(ok1465)* was generated by the *C. elegans* gene knockout consortium, and the Japanese National BioResource Project for *C. elegans* supplied *lat-2(tm463)* [both LG II]. The following extrachromosomal and integrated arrays were created for this study (Figure S8): *qaEx7513[lat-1(+) (pTL2) rol-6 (su1006)]*, *qaEx7515[lat-2p::gfp (pTL5) rol-6(su1006)]*, *qaIs7524[lat-1p::gfp (pTL13) rol-6(su1006)]*, *aprEx10,12,14,18[pax-3p::lat-1A (pSP14) rol-6 (su1006) pBSK]*, *aprEx20[lat-1(ΔRBL) (pSP8) rol-6(su1006) pBSK]*, *aprEx35-38,45[M05B5.2p::lat-1A (pTL24) rol-6(su1006) pBSK]*, *aprEx40[lat-1(ΔRBL 1-581)::gfp (pSP9) unc-119](+)]*, *aprEx77[lat-1::gfp (pSP5) rol-6(su1006) pBSK]*. The following alleles and transgenes have been previously described: *qIs56[lag-2p::gfp unc-119(+)]* (Kostić et al., 2003), *msIs114[rnt-1::gfp rol-6(+)]* (Kagoshima et al., 2005), *unc-119(ed3) ojIs1[unc-119(+) pie-1::GFP::tbb-2]* (Strome et al., 2001), *mom-2(t2180ts)* (Bischoff and Schnabel, 2006), *mom-2(or42)* (Thorpe et al., 1997), *mom-5(zu193)* (Rocheleau et al., 1997).

Transgenes and RNAi

Stably transmitting extrachromosomal array lines and integrants were generated by gonadal injection of the experimental construct DNA (1–2 ng/μl), the coinjection marker pRF4 [*rol-6(+)*] (100 ng/μl) or pDPMM016B[*unc-119(+)*] (60 ng/μl), and an empty pBluescript vector up to a final concentration of 120 ng/μl *unc-119(+)*. The *lat-1p::gfp* array was integrated by γ-irradiation.

DNA mixes containing *lat-1* rescuing constructs were injected in *lat-1 (ok1465)* heterozygotes balanced with *mIn1[mIs14 dpy-10(e128)]*, and transgenic individuals were isolated from F1 or F2 progeny. Multiple independent transgenic lines were established for each transgene tested. A construct was scored as nonrescuing when ten independent lines did not produce transgenic homozygotes.

RNAi of *lat-1* was carried out using feeding clone B0457.1 (II-6O04). F1 progeny of *lat-1(ok1465)* mutants were scored for enhancement of embryonic and larval arrest.

Developmental Arrest and Adult Brood Size

Embryonic and Larval Arrest Assay

Fifty young adult hermaphrodites per strain were allowed to lay eggs on NGM plates seeded with HB101 for 3 hr and then removed; embryos were washed off with 1 ml M9 buffer + 1% BSA (New England Biolabs), and 3–10 embryos per well were placed into 72-well flat-bottom Terasaki plates (Greiner Bio-One) with a mouth controlled pipette, incubated at 22°C, and scored on an inverted microscope 48 hr later.

Adult Brood Size

L4 hermaphrodites were placed on NGM plates seeded with HB101 and allowed to lay eggs. Every 24 hr the mother animal was transferred to a fresh plate until egg-laying ceased. Plates were incubated at 22°C and the number of adult animals was scored 48 hr after the mother was removed. All experiments were conducted at least in triplicate. Data were analyzed with an unpaired two-tailed t test for each genotype, and means are presented with SEM.

Microscopy

4D DIC imaging, lineage analysis, and quantitative evaluation of division plane angles were performed as described in Bischoff and Schnabel (2006) using SIMI Biocell software (SIMI Reality Motion Systems, Germany). Some DIC images were taken on a Leica DM RXA2 microscope. Confocal images were collected with Zeiss LSM5 and LSM510 Meta setups. Live imaging of developing transgenic embryos was conducted with a Deltavision Core (wide-field fluorescence deconvolution imaging system; Applied Precision Inc.). 4D stacks (spatial spacing: 0.2–0.5 μm; temporal spacing: 5–10 min) throughout morphogenesis were recorded simultaneously on 50–100 embryos using a motorized stage, and representative time points from exemplary embryos were chosen for deconvolution of fluorescent data stacks to limit exposure times during acquisition and aid image quality improvement. GFP::β-tubulin recordings were conducted using the same setup with different parameters (spatial spacing: 1.0 μm; temporal spacing: 60–90 s).

In Situ Hybridization and Immunohistochemistry

In situ hybridization analyses were performed as previously described (Tabara et al., 1996). The LAT-1 antiserum was generated by using purified LAT-1A RBL domain protein to raise polyclonal antibodies in rabbits (BioGenes, Berlin). Monospecific antigen-purified IgG fractions were used for immunostains. Immunostains of *C. elegans* embryos were essentially performed as described by Andrews and Ahringer (2007). Polyclonal rabbit-anti-LAT-1 antiserum was used 1:1000; monoclonal mouse-α-3NB12 (Priess and Thomson, 1987) was kindly provided by J. Ahringer and used 1:2. Secondary antibodies were from Molecular Probes and used 1:500.

SUPPLEMENTAL DATA

Supplemental Data include eight figures and Supplemental Experimental Procedures and can be found with this article online at http://www.cell.com/developmental-cell/supplemental/S1534-5807(09)00345-1/.

ACKNOWLEDGMENTS

We thank Jonathan Hodgkin, Alison Woollard, Iain Campbell, Julie Ahringer, Torsten Schöneberg, Sam Aparicio, Mark Carlton, and Johannes Grosse for their support, Eric Jorgensen, Morris Maduro, Ian Hope, and many more members of the *C. elegans* research community for generous sharing of mutants and other materials, and several colleagues for critical reading of the manuscript. This work was supported by grants from the Wellcome Trust (WT075336AIA), the BBSRC (BB/C504200/1), the EPA Cephalosporin Trust (CF077), and the Royal Society, and by DPhil studentships from the Wellcome Trust (T.L.), the Daimler-Benz Foundation (S.P.), the Algerian Ministry of Higher Education and Scientific Research (L.M.), and the BBSRC (H.W.-E.). T.L. and A.P.R. thank Richard Parton and Martin Anger for their advice and support with microscopy. Correspondence regarding NMR experiments should be addressed to I.V. (ioannis.vakonakis@psi.ch). I.V. acknowledges support from the Marie Curie Fellowships program and thanks the Royal Society for the automatic NMR sample changer grant.

Received: January 14, 2009
Revised: July 16, 2009
Accepted: August 24, 2009
Published: October 19, 2009

REFERENCES

Andrews, R., and Ahringer, J. (2007). Asymmetry of early endosome distribution in C. elegans embryos. PLoS ONE *2*, e493.

Bei, Y., Hogan, J., Berkowitz, L.A., Soto, M., Rocheleau, C.E., Pang, K.M., Collins, J., and Mello, C.C. (2002). SRC-1 and Wnt signaling act together to specify endoderm and to control cleavage orientation in early *C. elegans* embryos. Dev. Cell *3*, 113–125.

Bischoff, M., and Schnabel, R. (2006). A posterior centre establishes and maintains polarity of the Caenorhabditis elegans embryo by a Wnt-dependent relay mechanism. PLoS Biol. *4*, e396.

Brenner, S. (1974). The genetics of Caenorhabditis elegans. Genetics *77*, 71–94.

Carreira-Barbosa, F., Kajita, M., Morel, V., Wada, H., Okamoto, H., Martinez Arias, A., Fujita, Y., Wilson, S.W., and Tada, M. (2009). Flamingo regulates epiboly and convergence/extension movements through cell cohesive and signalling functions during zebrafish gastrulation. Development *136*, 383–392.

Chae, J., Kim, M.J., Goo, J.H., Collier, S., Gubb, D., Charlton, J., Adler, P.N., and Park, W.J. (1999). The Drosophila tissue polarity gene starry night encodes a member of the protocadherin family. Development *126*, 5421–5429.

Curtin, J.A., Quint, E., Tsipouri, V., Arkell, R., Cattanach, B., Copp, A., Henderson, D., Spurr, N., Stanier, P., Fisher, E., et al. (2003). Mutation of Celsr1 disrupts planar polarity of inner ear hair cells and causes severe neural tube defects in the mouse. Curr. Biol. *13*, 1129–1133.

Davies, B., Baumann, C., Kirchhoff, C., Ivell, R., Nubbemeyer, R., Habenicht, U.F., Theuring, F., and Gottwald, U. (2004). Targeted deletion of the epididymal receptor HE6 results in fluid dysregulation and male infertility. Mol. Cell. Biol. *24*, 8642–8648.

Goldstein, B. (1995). Cell contacts orient some cell division axes in the Caenorhabditis elegans embryo. J. Cell Biol. *129*, 1071–1080.

Goldstein, B., Takeshita, H., Mizumoto, K., and Sawa, H. (2006). Wnt signals can function as positional cues in establishing cell polarity. Dev. Cell *10*, 391–396.

Gomes, J.E., Encalada, S.E., Swan, K.A., Shelton, C.A., Carter, J.C., and Bowerman, B. (2001). The maternal gene spn-4 encodes a predicted RRM protein required for mitotic spindle orientation and cell fate patterning in early C. elegans embryos. Development *128*, 4301–4314.

Gönczy, P. (2008). Mechanisms of asymmetric cell division: flies and worms pave the way. Nat. Rev. Mol. Cell Biol. *9*, 355–366.

Gönczy, P., and Rose, L.S. (2005). Asymmetric cell division and axis formation in the embryo. In WormBook, The *C. elegans* Research Community, ed. 10.1895/wormbook.1.30.1, http://www.wormbook.org.

Gotta, M., and Ahringer, J. (2001). Distinct roles for Gα and Gβγ in regulating spindle position and orientation in Caenorhabditis elegans embryos. Nat. Cell Biol. *3*, 297–300.

Green, J.L., Inoue, T., and Sternberg, P.W. (2008). Opposing Wnt pathways orient cell polarity during organogenesis. Cell *134*, 646–656.

Guest, M., Bull, K., Walker, R.J., Amliwala, K., O'Connor, V., Harder, A., Holden-Dye, L., and Hopper, N.A. (2007). The calcium-activated potassium channel, SLO-1, is required for the action of the novel cyclo-octadepsipeptide anthelmintic, emodepside, in Caenorhabditis elegans. Int. J. Parasitol. *37*, 1577–1588.

Hadjantonakis, A.K., Formstone, C.J., and Little, P.F. (1998). mCelsr1 is an evolutionarily conserved seven-pass transmembrane receptor and is expressed during mouse embryonic development. Mech. Dev. *78*, 91–95.

Huang, S., Shetty, P., Robertson, S.M., and Lin, R. (2007). Binary cell fate specification during C. elegans embryogenesis driven by reiterated reciprocal asymmetry of TCF POP-1 and its coactivator beta-catenin SYS-1. Development *134*, 2685–2695.

Hutter, H., and Schnabel, R. (1994). glp-1 and inductions establishing embryonic axes in C. elegans. Development *120*, 2051–2064.

Hutter, H., and Schnabel, R. (1995a). Establishment of left-right asymmetry in the Caenorhabditis elegans embryo: a multistep process involving a series of inductive events. Development *121*, 3417–3424.

Hutter, H., and Schnabel, R. (1995b). Specification of anterior-posterior differences within the AB lineage in the C. elegans embryo: a polarising induction. Development *121*, 1559–1568.

Hutter, H., Vogel, B.E., Plenefisch, J.D., Norris, C.R., Proenca, R.B., Spieth, J., Guo, C., Mastwal, S., Zhu, X., Scheel, J., et al. (2000). Conservation and novelty in the evolution of cell adhesion and extracellular matrix genes. Science *287*, 989–994.

Kagoshima, H., Sawa, H., Mitani, S., Bürglin, T.R., Shigesada, K., and Kohara, Y. (2005). The C. elegans RUNX transcription factor RNT-1/MAB-2 is required for asymmetrical cell division of the T blast cell. Dev. Biol. *287*, 262–273.

Kaletta, T., Schnabel, H., and Schnabel, R. (1997). Binary specification of the embryonic lineage in Caenorhabditis elegans. Nature *390*, 294–298.

Kostić, I., Li, S., and Roy, R. (2003). cki-1 links cell division and cell fate acquisition in the C. elegans somatic gonad. Dev. Biol. *263*, 242–252.

Krasnoperov, V.G., Bittner, M.A., Beavis, R., Kuang, Y., Salnikow, K.V., Chepurny, O.G., Little, A.R., Plotnikov, A.N., Wu, D., Holz, R.W., et al. (1997). alpha-Latrotoxin stimulates exocytosis by the interaction with a neuronal G-protein-coupled receptor. Neuron *18*, 925–937.

Lambie, E.J., and Kimble, J. (1991). Two homologous regulatory genes, lin-12 and glp-1, have overlapping functions. Development *112*, 231–240.

Lawrence, P.A., Struhl, G., and Casal, J. (2007). Planar cell polarity: one or two pathways? Nat. Rev. Genet. *8*, 555–563.

Lin, R., Hill, R.J., and Priess, J.R. (1998). POP-1 and anterior-posterior fate decisions in *C. elegans* embryos. Cell *92*, 229–239.

Lin, H.H., Chang, G.W., Davies, J.Q., Stacey, M., Harris, J., and Gordon, S. (2004). Autocatalytic cleavage of the EMR2 receptor occurs at a conserved G protein-coupled receptor proteolytic site motif. J. Biol. Chem. *279*, 31823–31832.

Mango, S.E., Thorpe, C.J., Martin, P.R., Chamberlain, S.H., and Bowerman, B. (1994). Two maternal genes, apx-1 and pie-1, are required to distinguish the fates of equivalent blastomeres in the early Caenorhabditis elegans embryo. Development *120*, 2305–2315.

Mee, C.J., Tomlinson, S.R., Perestenko, P.V., De Pomerai, D., Duce, I.R., Usherwood, P.N., and Bell, D.R. (2004). Latrophilin is required for toxicity of black widow spider venom in Caenorhabditis elegans. Biochem. J. *378*, 185–191.

Mizumoto, K., and Sawa, H. (2007). Two betas or not two betas: regulation of asymmetric division by beta-catenin. Trends Cell Biol. *17*, 465–473.

Nordström, K.J., Lagerström, M.C., Wallér, L.M., Fredriksson, R., and Schiöth, H.B. (2008). The Secretin GPCRs descended from the family of Adhesion GPCRs. Mol. Biol. Evol. *26*, 71–84.

Park, F.D., and Priess, J.R. (2003). Establishment of POP-1 asymmetry in early C. elegans embryos. Development *130*, 3547–3556.

Park, F.D., Tenlen, J.R., and Priess, J.R. (2004). C. elegans MOM-5/frizzled functions in MOM-2/Wnt-independent cell polarity and is localized asymmetrically prior to cell division. Curr. Biol. *14*, 2252–2258.

Piao, X., Hill, R.S., Bodell, A., Chang, B.S., Basel-Vanagaite, L., Straussberg, R., Dobyns, W.B., Qasrawi, B., Winter, R.M., Innes, A.M., et al. (2004). G protein-coupled receptor-dependent development of human frontal cortex. Science *303*, 2033–2036.

Priess, J.R. (2005). Notch signaling in the C. elegans embryo. In WormBook, The *C. elegans* Research Community, ed. 10.1895/wormbook.1.4.1, http://www.wormbook.org.

Priess, J.R., and Thomson, J.N. (1987). Cellular interactions in early *C. elegans* embryos. Cell *48*, 241–250.

Priess, J.R., Schnabel, H., and Schnabel, R. (1987). The glp-1 locus and cellular interactions in early *C. elegans* embryos. Cell *51*, 601–611.

Rocheleau, C.E., Downs, W.D., Lin, R., Wittmann, C., Bei, Y., Cha, Y.H., Ali, M., Priess, J.R., and Mello, C.C. (1997). Wnt signaling and an APC-related gene specify endoderm in early *C. elegans* embryos. Cell *90*, 707–716.

Schlesinger, A., Shelton, C.A., Maloof, J.N., Meneghini, M., and Bowerman, B. (1999). Wnt pathway components orient a mitotic spindle in the early *Caenorhabditis elegans* embryo without requiring gene transcription in the responding cell. Genes Dev. *13*, 2028–2038.

Schnabel, R. (1997). Why does a nematode have an invariant cell lineage? Semin. Cell Dev. Biol. *8*, 341–349.

Schnabel, R., Hutter, H., Moerman, D., and Schnabel, H. (1997). Assessing normal embryogenesis in *Caenorhabditis elegans* using a 4D microscope: variability of development and regional specification. Dev. Biol. *184*, 234–265.

Shima, Y., Kengaku, M., Hirano, T., Takeichi, M., and Uemura, T. (2004). Regulation of dendritic maintenance and growth by a mammalian 7-pass transmembrane cadherin. Dev. Cell *7*, 205–216.

Siller, K.H., and Doe, C.Q. (2009). Spindle orientation during asymmetric cell division. Nat. Cell Biol. *11*, 365–374.

Steinel, M.C., and Whitington, P.M. (2009). The atypical cadherin Flamingo is required for sensory axon advance beyond intermediate target cells. Dev. Biol. *327*, 447–457.

Strome, S., Powers, J., Dunn, M., Reese, K., Malone, C.J., White, J., Seydoux, G., and Saxton, W. (2001). Spindle dynamics and the role of gamma-tubulin in early *Caenorhabditis elegans* embryos. Mol. Biol. Cell *12*, 1751–1764.

Strutt, D. (2008). The planar polarity pathway. Curr. Biol. *18*, R898–R902.

Südhof, T.C. (2001). alpha-Latrotoxin and its receptors: neurexins and CIRL/latrophilins. Annu. Rev. Neurosci. *24*, 933–962.

Sulston, J.E., Schierenberg, E., White, J.G., and Thomson, J.N. (1983). The embryonic cell lineage of the nematode *Caenorhabditis elegans*. Dev. Biol. *100*, 64–119.

Tabara, H., Motohashi, T., and Kohara, Y. (1996). A multi-well version of in situ hybridization on whole mount embryos of *Caenorhabditis elegans*. Nucleic Acids Res. *24*, 2119–2124.

Thorpe, C.J., Schlesinger, A., Carter, J.C., and Bowerman, B. (1997). Wnt signaling polarizes an early *C. elegans* blastomere to distinguish endoderm from mesoderm. Cell *90*, 695–705.

Tissir, F., Bar, I., Jossin, Y., De Backer, O., and Goffinet, A. (2005). Protocadherin Celsr3 is crucial in axonal tract development. Nat. Neurosci. *8*, 451–457.

Usui, T., Shima, Y., Shimada, Y., Hirano, S., Burgess, R.W., Schwarz, T.L., Takeichi, M., and Uemura, T. (1999). Flamingo, a seven-pass transmembrane cadherin, regulates planar cell polarity under the control of Frizzled. Cell *98*, 585–595.

Vakonakis, I., Langenhan, T., Prömel, S., Russ, A., and Campbell, I.D. (2008). Solution structure and sugar-binding mechanism of mouse latrophilin-1 RBL: a 7TM receptor-attached lectin-like domain. Structure *16*, 944–953.

Veninga, H., Becker, S., Hoek, R.M., Wobus, M., Wandel, E., van der Kaa, J., van der Valk, M., de Vos, A.F., Haase, H., Owens, B., et al. (2008). Analysis of CD97 expression and manipulation: antibody treatment but not gene targeting curtails granulocyte migration. J. Immunol. *181*, 6574–6583.

Walston, T.D., and Hardin, J. (2006). Wnt-dependent spindle polarization in the early C. elegans embryo. Semin. Cell Dev. Biol. *17*, 204–213.

Walston, T., Tuskey, C., Edgar, L., Hawkins, N., Ellis, G., Bowerman, B., Wood, W., and Hardin, J. (2004). Multiple Wnt signaling pathways converge to orient the mitotic spindle in early *C. elegans* embryos. Dev. Cell *7*, 831–841.

Willson, J., Amliwala, K., Davis, A., Cook, A., Cuttle, M.F., Kriek, N., Hopper, N.A., O'Connor, V., Harder, A., Walker, R.J., et al. (2004). Latrotoxin receptor signaling engages the UNC-13-dependent vesicle-priming pathway in *C. elegans*. Curr. Biol. *14*, 1374–1379.

Zallen, J.A. (2007). Planar polarity and tissue morphogenesis. Cell *129*, 1051–1063.